
Modelling of the colloid facilitated actinide transport in the geosphere with the computer code TRAPIC

U. Noseck

*Gesellschaft für Anlagen-und Reaktorsicherheit (GRS) mbH - Theodor-Heuss-Str. 4
38122 Braunschweig – Germany*

Abstract: The computer code TRAPIC (**T**ransport of **P**ollutants **I**nfluenced by **C**olloids) was developed to simulate one or two-dimensional colloid facilitated contaminant transport in porous media. The colloids are considered to be dissolved in the aqueous phase or attached on retention sites of the matrix. For the contaminants four different phases are considered: dissolved in the aqueous phase, sorbed on mobile colloids, sorbed on the surface of the aquifer material, or sorbed on immobile colloids. The mass exchange between the corresponding phases is modelled by kinetically controlled sorption and filtration processes. Sorption processes of the contaminants can be described by Henry, Langmuir or Freundlich reactions.

The transport code TRAPIC has been applied to describe the Eu migration in column experiments with humic-rich groundwater. Good agreement is obtained by simulating the migration experiments with sorption parameters taken from batch experiments and from literature. The transport in the 10 m column can be described using the same simulation parameters as for the 50 cm columns. Details of the transport code TRAPIC and simulation results of the Eu-transport in column experiments are shown. Furthermore, first calculations concerning the impact of colloids on long-term safety assessment of a repository for radioactive waste are presented.

1. INTRODUCTION

Organic and inorganic colloids are present in various concentrations in natural groundwaters [1]. From field studies it is known, that colloids can have a strong impact on the transport of pollutants, since they migrate at velocities similar to the groundwater velocity and act as a carrier by sorbing a significant amount of contaminants [2]. This process can be of importance for the long-term safety of underground repositories, where the geosphere is usually considered as a significant barrier for contaminants, due to high sorption capacities of the sediments for many elements. Rather high concentrations of humic colloids up to 200 mg DOC/l have been observed in the overburden of the salt dome in Gorleben [3]. According to measurements of concentrations and ages of humics in real aquifer systems (Franconian Albvorland, Gorleben) there is evidence for the stability and transport of humic colloids over large distances [4].

Several column experiments with DOC rich water have been performed up to now to investigate the impact of humic colloids on the actinide transport (e.g. [5,6]). Emphasis was attached to the influence of flow-velocity, column length and different sediments. The results indicate that kinetic controlled sorption processes play an essential role. In order to describe

the colloid facilitated transport in performance assessment the computer code TRAPIC was developed [7].

The aim of this study is to show the applicability of the code TRAPIC to model the colloid facilitated transport in column experiments. A number of europium-humate migration experiments in different sandy sediments, which were performed by Klotz et al. [8,9], are simulated. The relevant kinetic controlled sorption mechanisms can be identified and values for the sorption rates are estimated. The results are compared with those of previous investigations.

In the second part of this paper first results from calculations with simplified models for performance assessment based on the present-day knowledge were presented. The aim was to investigate the impact of humic colloid facilitated transport of actinides in the far field of a repository on the basis of the present day knowledge. This exemplary study [10] has been performed for typical conditions expected in a repository in salt rock in Northern Germany [11].

2. DESCRIPTION OF THE EUROPIUM MIGRATION EXPERIMENTS

The migration of Eu(III) through columns filled with five different sandy sediments were investigated by Klotz et al. [9]. In all experiments the same humic rich groundwater with a concentration of 80 mg DOC/l was used. The columns were equilibrated with the groundwater for about three months. Before injection into the column the groundwater was equilibrated with Eu(III) for some weeks. After equilibration an amount of 98 % Eu was bound to colloidal humic particles. Typical colloid sizes are in the range of 1 to 200 nm.

In order to investigate the influence of groundwater flow the experiment with each sediment was performed at three different Darcy-velocities. The column length is 0.5 m with a diameter of 0.05 m. The hydraulic properties of the columns were determined by use of ³H₂O-tracers. The sediment properties and information on hydraulic conditions are listed in table 1.

Furthermore batch experiments with the same sediment-groundwater systems were carried out to investigate the equilibrium sorption of europium.

Table 1. Sediment and hydraulic properties

	1	2	3	4	5
sediment	coarse sand	Fine sand	fine sand	medium sand	coarse sand
effective porosity Θ	0.05	0.29	0.290	0.261	0.283
dispersion length [10^{-3} m]	120 - 220	1.2 - 1.5	1.4 - 2.2	2.5 - 2.9	3.1 - 3.4
Darcy-velocity [10^{-3} m/h]					
high	36.7	35.2	37.1	37.1	37.1
medium	8.35	8.17	8.21	8.64	8.50
low	1.71	1.65	1.13	1.74	1.68
sorption value R_d [ml/g] from Batch experiment	3.3	6.0	3.9	0.8	0.4

The main characteristics of the experimental results can be summarised as follows:

- the Eu-tracer is transported as fast as the ideal tracer ³H₂O, although the distribution coefficients measured in batch experiments indicate a stronger sorption,
- the recoveries are between 0.6 and 0.95 and decrease with increasing travel time (see fig. 1),
- the breakthrough curves show significant tailing.

The simulation results for these new experiments will be compared with two previous works [7], [13]: *pE-0.5m* denotes a similar experiment performed in 0.5 m columns and *pE-10m*

denotes an experiment with a 10 m long column. In both of the experiments sediment 2 was used.

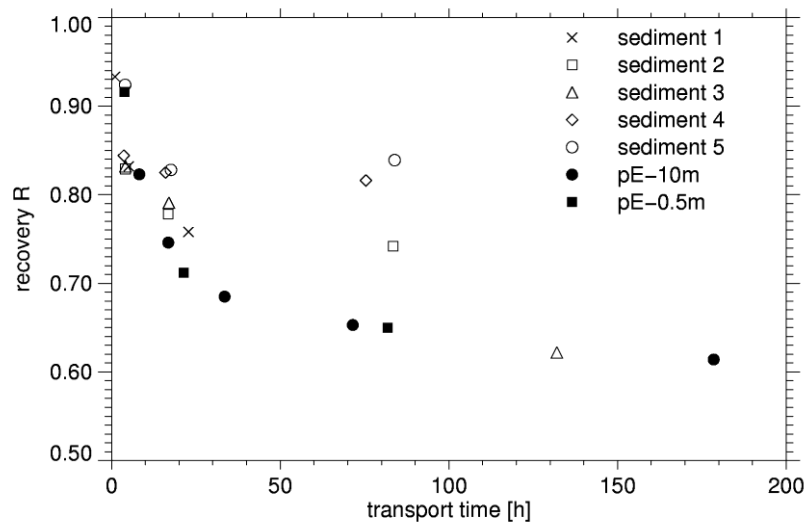


Figure 1. Recoveries versus transport time

3. DESCRIPTION OF THE MODEL

The computer code TRAPIC (**T**ransport of **P**ollutants **I**nfluenced by **C**olloids) considers one- or two-dimensional colloid transport in porous media. The model is schematically shown in figure 2. The colloids are considered to be dissolved in the aqueous phase or attached on retention sites of the sediment matrix. The europium is assumed to be mobile – dissolved or sorbed on mobile colloids - or immobile – sorbed on the sediment or sorbed on immobile colloids. TRAPIC was already described in previous publications [7], [12].

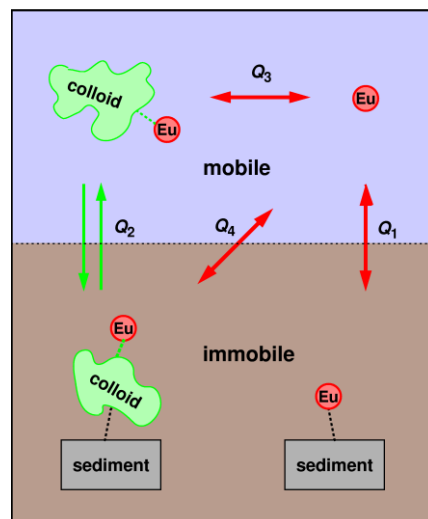


Figure 2. Schematic representation of the model

The mass balance equations for the contaminants are written as

$$\begin{aligned}
 \frac{\partial}{\partial t} \left(\Theta C_{Pf} \right) + \nabla \cdot \left[\bar{q}_p C_{Pf} - \Theta D_p \nabla C_{Pf} \right] &= -Q_1^p - Q_3^p - Q_4^p \\
 \frac{\partial}{\partial t} \left(\Theta S_{Pf} \right) &= Q_1^p, \\
 \frac{\partial}{\partial t} \left(\Theta C_{Pb} \right) + \nabla \cdot \left[\bar{q}_c C_{Pb} - \Theta D_c \nabla C_{Pb} \right] &= -Q_2^p + Q_3^p, \\
 \frac{\partial}{\partial t} \left(\Theta S_{Pb} \right) &= Q_2^p + Q_4^p,
 \end{aligned} \tag{1}$$

where C_{Pf} [ML⁻³] denotes the dissolved contaminant concentration, C_{Pb} [ML⁻³] and S_{Pb} [ML⁻³] the concentration of contaminants sorbed on mobile and immobile colloids, respectively, and S_{Pf} [MM⁻¹] the contaminant concentration sorbed on the sediment. The tensors D_p and D_c [L²T⁻¹] describe the diffusion- and dispersion effects of the contaminants and colloids, whereas the Darcy velocities are given by \bar{q}_p and \bar{q}_c [LT⁻¹]. Q_1^p [ML⁻³T⁻¹] describes the contaminant sediment interaction, Q_3^p [ML⁻³T⁻¹] and Q_4^p [ML⁻³T⁻¹] determine the interaction of dissolved contaminants between mobile and immobile colloids, respectively. The source term Q_2^p [ML⁻³T⁻¹] gives the change of contaminant concentration due to reversible interactions of the colloids with the sediment.

The sorption of contaminants on the colloids and on the sediment is described by Langmuir isotherms:

$$\begin{aligned}
 C_{Pb} &= C_c f_3 \left(C_{Pf} \right) = C_c \frac{\beta_3 \kappa_3 C_{Pf}}{1 + \beta_3 C_{Pf}}, \\
 S_{Pb} &= C_c f_4 \left(C_{Pf} \right) = S_c \frac{\beta_4 \kappa_4 C_{Pf}}{1 + \beta_4 C_{Pf}}, \\
 S_{Pf} &= f_1 \left(C_{Pf} \right) = \frac{b_1 \kappa_1 C_{Pf}}{1 + b_1 C_{Pf}}.
 \end{aligned} \tag{2}$$

C_c [ML⁻³] and S_c [ML⁻³] denotes the concentration of mobile and immobile colloids, S_{Pf} [ML⁻³] denotes the concentration of immobile contaminants, β_3 and β_4 [L³M⁻¹] are the complexing constants, κ_3 and κ_4 [MM⁻¹] are the sorption capacities of the colloids for contaminants, b_1 is the Langmuir coefficient and κ_1 the sorption capacity of the sediment for contaminants. The interaction processes are governed by kinetic Langmuir-reactions and are as follows:

$$\begin{aligned}
 Q_1^p &= k_1 \rho \left[f_1 \left(C_{Pf} \right) - S_{Pf} \right], \\
 Q_3^p &= k_3 \Theta \left[f_3 \left(C_{Pf} \right) - C_{Pb} \right], \\
 Q_4^p &= k_4 \left[f_4 \left(C_{Pf} \right) - S_{Pb} \right].
 \end{aligned} \tag{3}$$

The interaction of colloids with the sediment was assumed to be of first order kinetics

$$Q_2^p = K_2 \Theta = k_2 \rho_c S_c, \tag{4}$$

with the effective porosity Θ and the capture and release constants K_2 and k_2 [T⁻¹]. Consistent to this the change of the contaminant concentration caused by colloid sediment interactions is

$$Q_2^p = K_2 \Theta C_{pb} - k_2 S_{pb} \cdot \quad (5)$$

A common approach to describe the deep bed filtration neglecting the remobilization of filtered colloids leads to

$$K_2 \Theta = |q_c| \lambda_f \alpha \cdot \quad (6)$$

The filter coefficient λ_f can be defined as [14]

$$\lambda_f = \frac{3}{2} \frac{1-n}{d_c} \eta \cdot \quad (7)$$

η denotes the collection efficiency and α the attachment factor describing the part of the colloid matrix collisions leading to binding. According to approaches of Tien et al. [14] and Yao et al. [15] the collection efficiency can be divided into diffusion, sedimentation and mechanical filtration processes. On the conditions of the considered experiments, the filtration is dominated by the diffusion process. This can be described according to Yao :

$$\eta = 0.9 \left(\frac{kT}{\mu d_p d_c q_c} \right)^{2/3}, \quad (8)$$

with the diameter of the colloidal particles d_p , the pore diameter d_c and the dynamic viscosity μ .

4. SIMULATION

The simulation of the europium-humate-experiments was performed similar to earlier studies with sediment 2 [7,12,13].

Sensitivity analyses show that recoveries <100% are due to irreversible filtration and/or desorption of Eu from colloids followed by sorption on the sediment matrix [2]. Investigations of *Schüßler et al.* indicate that the latter process plays the predominant role in column experiments with actinide-humate complexes [16]. In that case the desorption rate k_3 of the colloid bound europium determines the Eu recovery. Accordingly, k_3 is obtained from simulation.

The observed tailing of the breakthrough curve indicates reversible interactions between sediment matrix and the colloids. The capture rate, describing the dynamics of the process of colloids getting into contact with the sediment, depends according to filtration theory on the porosity and the flow velocity of the colloids (cp equations 6 and 7). Therefore, varying rates K_2 are expected for the different experiments. The K_2 values are derived by fitting the tailing of the breakthrough curve. Then k_2 yields to $K_2 \Theta (C_{col} / \rho_c S_{col})$. On the assumption of a constant mobile colloid concentration the ratio K_2 / k_2 determines the immobile colloid concentration. The value K_2 / k_2 was obtained as best fit from the migration experiment with sediment 2 and was held constant for the simulation of all other experiments. Therewith the fraction of immobile colloids is determined to about 20%.

For the simulation hydraulic data listed in table 1 are used. In some cases the Darcy-velocities were moderately corrected, since small differences between the arrival time of ^3HHO and Eu are observed, which are assumed to be due to heterogeneities in the column. Further input data are listed in table 2 and 3. These data stem from independent batch experiments, and from literature, respectively. For details, see [12] and [13]. According to the R_d -values measured in batch experiments (cp table 1) and on the assumption of a constant mobile colloid concentration the Langmuir coefficients shown in table 3 were estimated.

Table 2. Parameter values for the simulation

column length l	0.5 m
column diameter d	0.05 m
injected volume of Eu-tracer solution V_p	1 ml
injected Eu-concentration $C_{Pf,0}$	$0.045 \cdot 10^{-3} \text{ g l}^{-1}$
injected Eu-Humate concentration $C_{Pb,0}$	$2.205 \cdot 10^{-3} \text{ g l}^{-1}$
density of the sediment ρ	2600 kg m^{-3}
density of the colloids ρ_C	1200 kg m^{-3}
diffusion coefficient of the colloids D_m^C	$10^{-11} \text{ m}^2 \text{ s}^{-1}$
diffusion coefficient of the pollutants D_m^P	$10^{-11} \text{ m}^2 \text{ s}^{-1}$
dynamic viscosity μ	$0.086 \text{ g m}^{-1} \text{ s}^{-1}$
pore diameter d_C	$2 \cdot 10^{-4} \text{ m}$
Langmuir coefficient b_1	s. table 3
sorption capacity κ_1	$3.3 \cdot 10^{-3} \text{ kg kg}^{-1}$
complexation constant $\beta_3 = \beta_4$	$5.23 \cdot 10^{-4} \text{ l mol}^{-1}$
loading capacity $\kappa_3 = \kappa_4$	$1.787 \text{ mol kg}^{-1}$
concentration of mobile colloids C_C	0.08 g l^{-1}
concentration of immobile colloids $\rho_C S_C$	$3.84 \cdot 10^{-3} \text{ g l}^{-1}$
sorption rate k_1	$>1.4 \cdot 10^{-4} \text{ s}^{-1}$

Table 3: Langmuir coefficients used for simulation

	Langmuir coefficient b_1 [$\text{m}^3 \text{ g}^{-1}$]
experiment 1	0.250
experiment 2	0.496
experiment 3	0.320
experiment 4	0.066
experiment 5	

5. RESULTS AND DISCUSSION

As described above for simulation of the column experiments only the rates k_3 and K_2 were fitted. Exemplary the breakthrough curves for sediment 3 are shown in figure 3. All experiments with sediments 2, 3, 4 and 5 are in a good agreement with the simulations. For sediment 1 some slight deviations in the tailing of the breakthrough curve between experiment and simulation occur, which have to be further investigated.

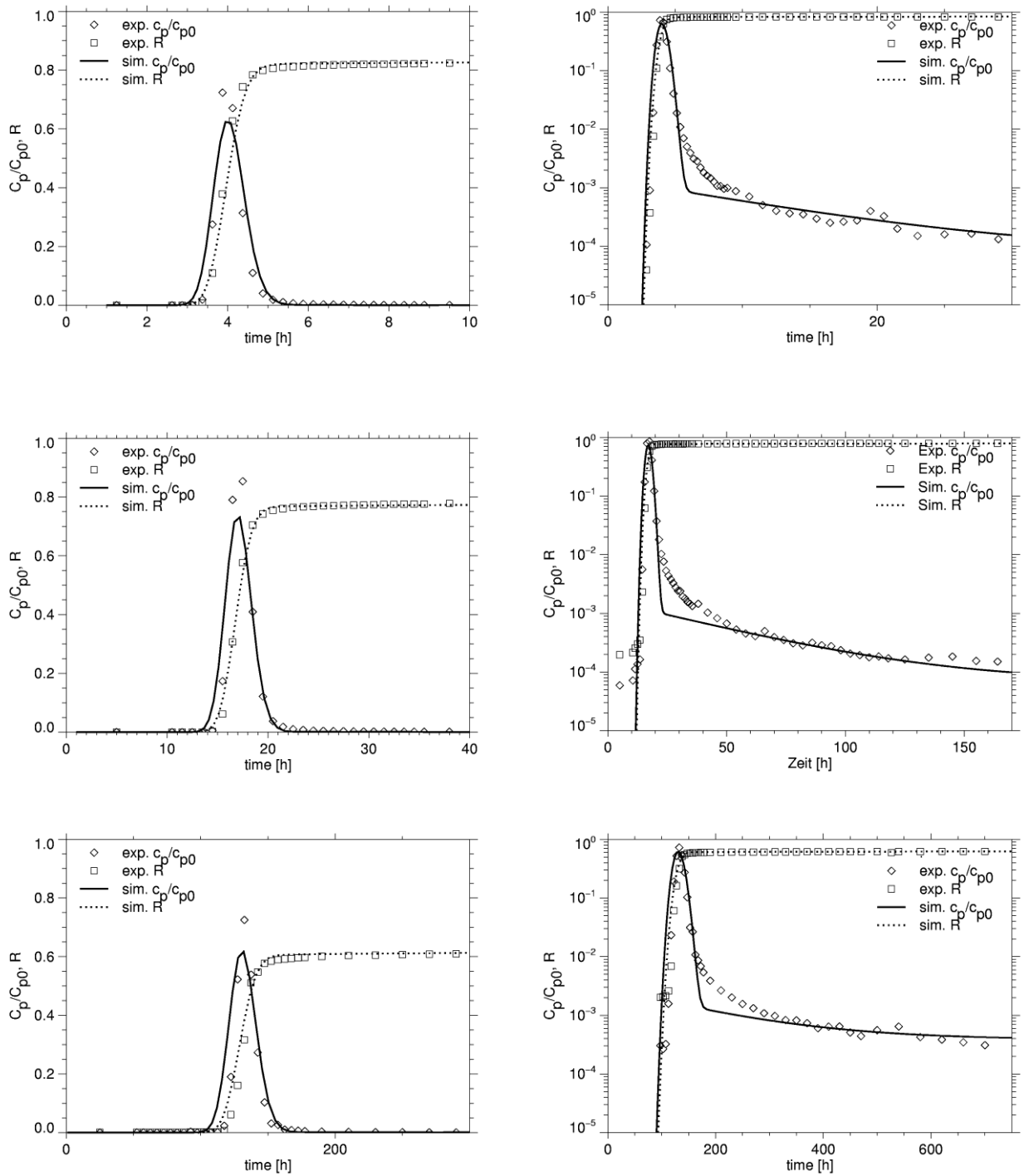


Figure 3. Best fit and experimentally observed curves for sediment 3 in linear (left) and logarithmic (right) presentation for various Darcy velocities. C_p/C_{p0} represents the normalised concentration. Top: Darcy-velocity $q = 37 \cdot 10^{-3}$ m/h, middle: $q = 8.2 \cdot 10^{-3}$ m/h, bottom: $q = 1.1 \cdot 10^{-3}$ m/h.

Figure 4 shows the effective desorption rates k_3 obtained by simulation plotted versus the transport time of Eu-humate. Besides the results of this work, the values received in earlier investigations for 0.5 m and 10 m columns are included. The desorption rates decrease exponentially with transport time. The values received in this study agree well with those determined in previous investigations.

The mechanisms, which are responsible for the decrease of the desorption rate with increasing travel time are still under investigation, e.g. Schüßler et al. [16].

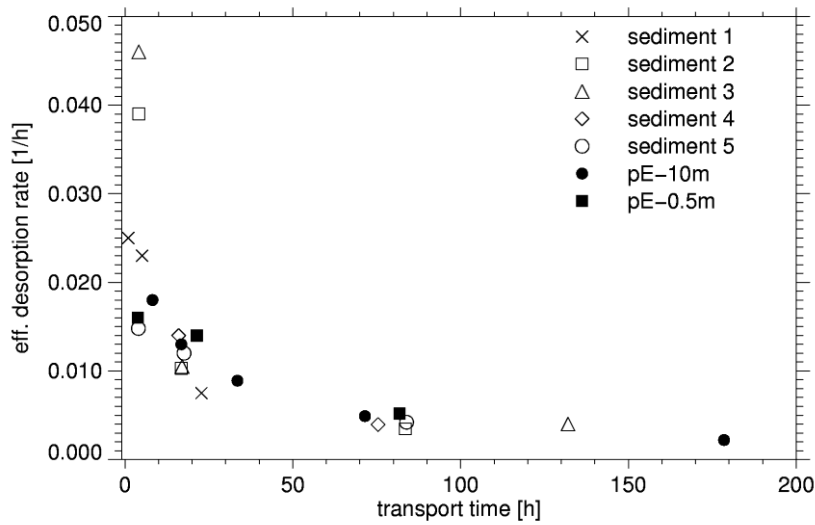


Figure 4: effective desorption rates k_3 as a function of transport time

K_2 rates are derived by simulations of the tailing of the breakthrough curves. In Figure 5 the sorption rates ΘK_2 obtained by best fits are plotted versus Darcy-velocity and are compared with results obtained from filtration theory. The error bars represent the values for $q\lambda_f\alpha$ calculated by the approach of Yao (see equations 7 and 8) considering an uncertainty of colloid size between 1 and 200 nm. An average porosity of 0.27 and an attachment factor of $2 \cdot 10^{-5}$ were assumed. The capture rates increase with increasing Darcy-velocity and are in the same order of magnitude as expected by filtration theory.

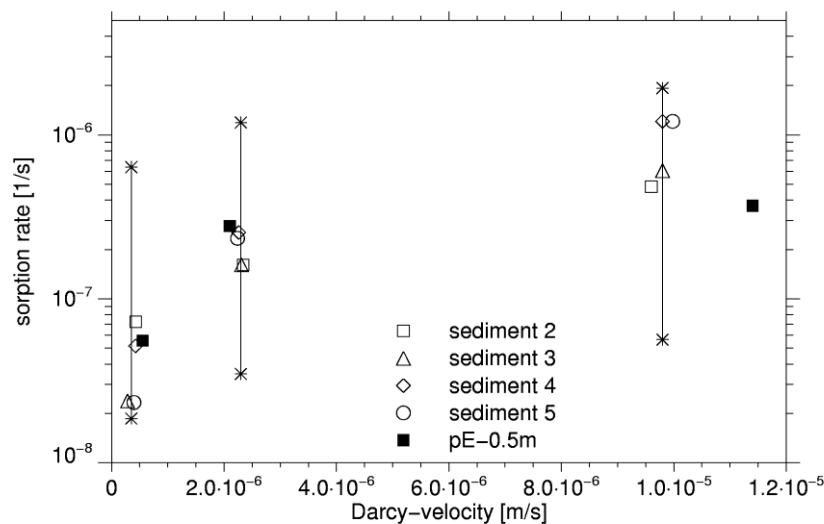


Figure 5: Sorption rates from simulation ($K_2\Theta$) and theory ($\Theta=0.27$, $\alpha=2 \cdot 10^{-5}$). The error bars represent the values for $q\lambda_f\alpha$ considering an uncertainty of colloid size from 1 to 200 nm.

6. APPLICATION TO PERFORMANCE ASSESSMENT

Besides the europium migration experiments, a lot more detailed investigations on humic colloid facilitated actinide transport are currently performed, eg. [3-6, 16].

A crucial question for performance assessment is the upscaling of the results, i.e. whether the effective desorption rate of the actinides from the colloids further decreases with increasing travel time and whether a certain amount of the actinides might stay irreversibly bound on colloids, during transport through the geosphere. Since this cannot be ruled out at the present day knowledge, the effect has been investigated in a study with simplified models for humic colloid facilitated transport in performance assessment. This study is described in detail in [10]. In the following, the results will be shortly summarized.

6.1 Assumptions

Calculations were performed based on a typical scenario for a radioactive waste repository in a salt formation [11]. The impact of the colloids was regarded in the far-field transport of the repository. The results are compared to a reference case, where linear equilibrium sorption of the actinides was considered. The influence of humic colloids on the migration behaviour of the actinides thorium, uranium, americium, curium, plutonium and neptunium was investigated for two different cases: In the first case a part of the actinides is irreversibly bound to mobile colloids, in the second case a kinetically controlled desorption process is considered.

Generally it was assumed that the humic colloids do not interact with the sediment, i.e. they are transported without sorption or filtration through the whole model area. A consistent description of batch and column experiments investigating the actinide migration behaviour is available only for Am(III). Exemplary, these data were used for all actinides.

Eu(III) batch desorption experiments with natural humic substances (humic colloid concentration of $2\text{-}6\cdot 10^{-4}$ eq dm⁻³) show that within 100 days only 55 % of the initially humic bound Eu(III) can be desorbed

[17]. Considering Eu(III) as a homologue for Am(III), it can be assumed that 45 % of Am(III) is irreversibly bound on humic colloids. Calculations were performed assuming a fraction of 45 % actinides irreversibly bound to humic colloids.

From column experiments it became evident that desorption kinetics of actinides from humic colloids are rather slow. Concerning the kinetically controlled desorption, the desorption rate of actinides from the humic colloids has been varied, keeping all other parameters constant. As lowest desorption rate a value of 7.0 y^{-1} observed in laboratory experiments with natural occurring Eu(III) humic complexes [17] has been applied. Three calculations with further reduced desorption rates are performed to show the impact of this time dependent process.

6.2 Results

In Fig. 6 the results for the reference case are shown. In the reference case humic colloids are not considered. The radionuclide retardation is calculated using the K_d -concept [10]. The maximum annual radiation exposure is mainly determined by the fission products ⁷⁹Se, ¹²⁹I, and ¹³⁵Cs. The radiation exposure caused by the actinides is more than one order of magnitude lower and is made up by ²²⁶Ra and ²³⁷Np. The relatively short lived actinides as e.g. ²⁴¹Pu and ²⁴¹Am with half-lives of 14.4 and 432.5 years, respectively, do not play a role since they are strongly sorbed and have already decayed during transport through the far field.

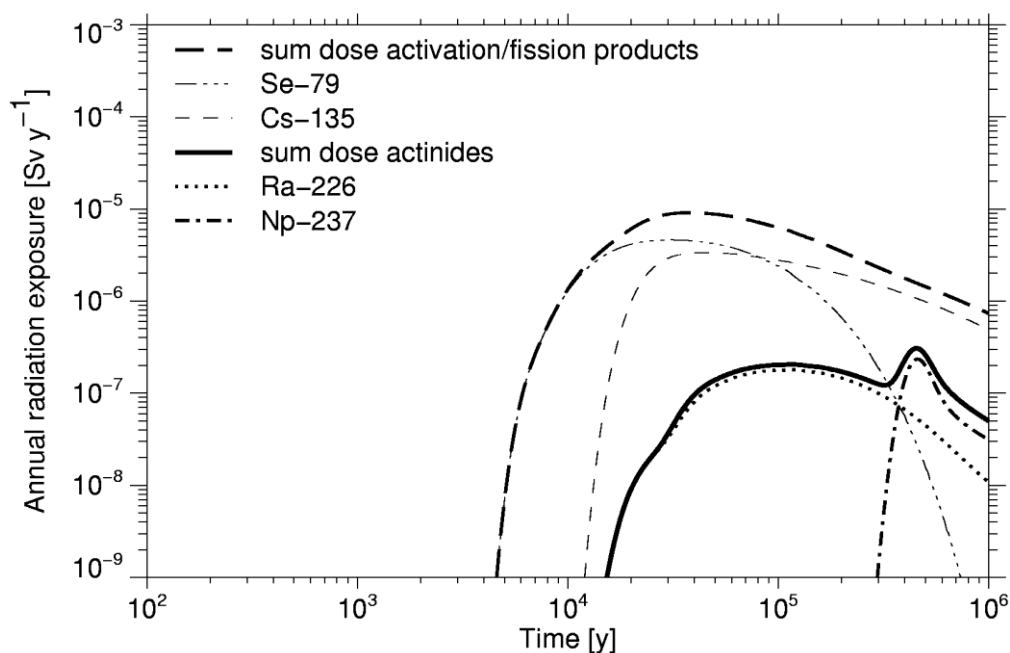


Fig. 6: Annual radiation exposure for the reference case (humic colloids are not considered)

6.3. Irreversibly bound fraction

Figure 7 demonstrates the impact of an irreversibly bound actinide fraction which is assumed to migrate without retardation through the far field. The main effect is an increase in radiation exposure at early times after about 10^3 years. Considering 45 % of the actinides bound to humic colloids, the maximum radiation exposure due to actinides increases by more than two orders of magnitude compared to the actinide curve in the reference case. As shown in the bottom part of the figure the rather short lived radionuclides ^{241}Am and ^{243}Am are dominating the annual radiation exposure between 10^3 and 10^5 years. In the reference case these nuclides are fully decayed during far-field transport, since their travel times exceeds their half lives by orders of magnitude.

Obviously, the effect is linearly proportional to the irreversibly bound fraction, which is seen by comparison with the curve of only 2 % irreversibly bound actinides. The maximum radiation exposure of the "2 % curve" is by a factor of 22.5 lower, but still a factor 8 higher than those from the actinides in the reference case.

The consequence is less dramatic in case of long-lived and medium sorbing radionuclides like ^{237}Np . The first maximum (A) of ^{237}Np at about $2 \cdot 10^3$ years caused by the colloid bound fraction is only slightly higher than the peak (B) at $4.5 \cdot 10^5$ years caused by a reversibly sorbed Np (cp. figure 3, bottom). This is due to the long half live of ^{237}Np of $2.1 \cdot 10^6$ years. At the time of maximum of about $5 \cdot 10^5$ years only a small amount is decayed. Since the radionuclide source can be considered nearly constant over the migration time for ^{237}Np , there is additionally only a small effect of longitudinal dispersion, which would lead to a decrease in concentration.

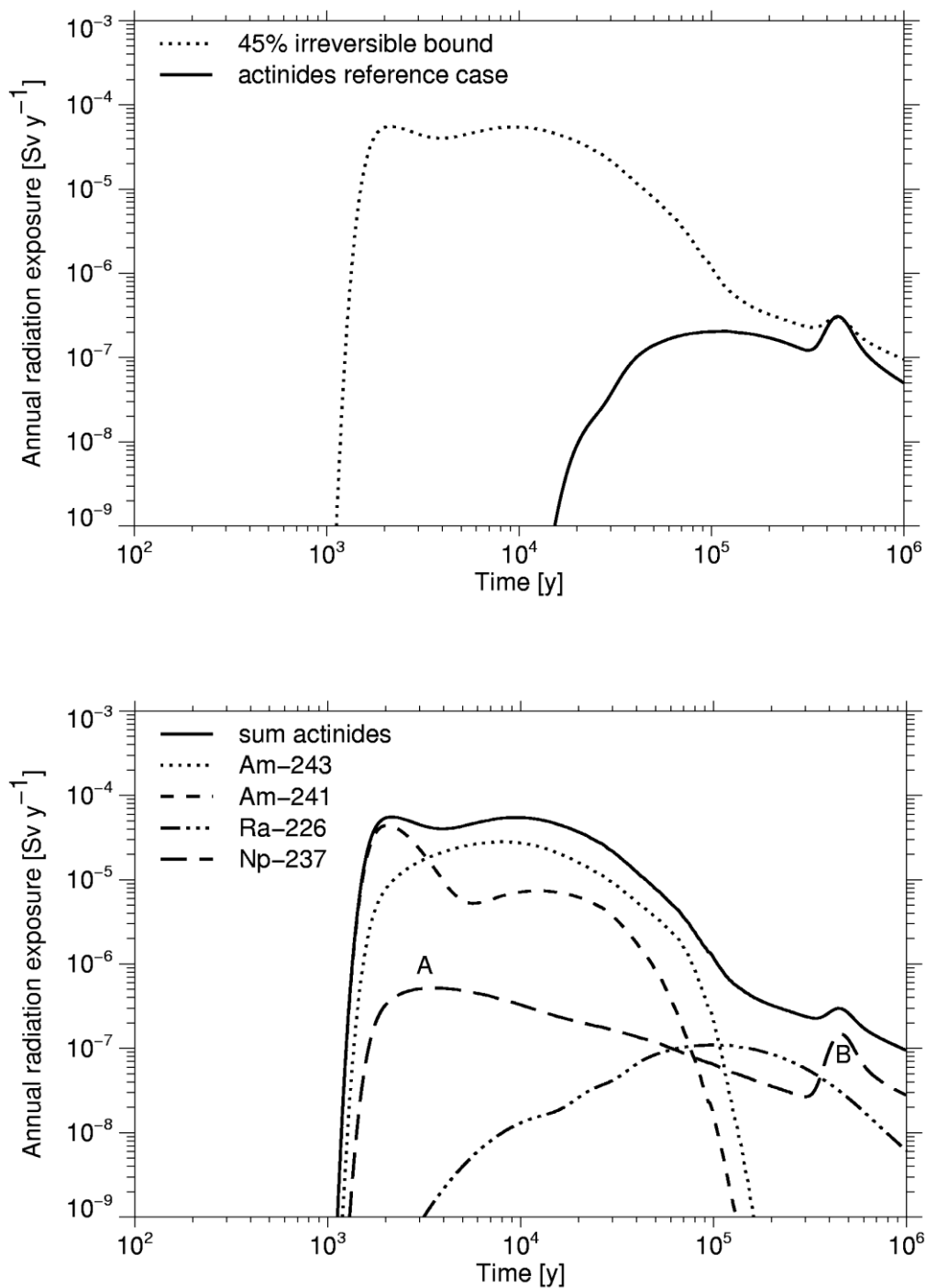


Figure 7: Top: Annual Radiation exposure due to the sum of all actinides. Bottom: Contribution of the most relevant actinides to the maximum annual radiation exposure (45 % irreversibly bound).

6.4. Desorption kinetics

As shown in table 3, calculations with four different rate constants for the desorption of actinides from the humic colloids have been carried out. Figure 8 shows the annual radiation exposure obtained for the different cases. Case A represents the desorption rate of 7.0 y⁻¹ corresponding to the lowest value

observed in laboratory experiments with natural occurring Eu(III)-humic [17]. The curve is identical to the one calculated for the reference case. This means, on the assumed hydrological conditions the desorption rate of 7.0 y^{-1} still represents an equilibrium

process. And also if the desorption rate is decreased by a factor of 100 (case B) the curve still does not differ from the one of the reference case.

A desorption rate of $7 \cdot 10^{-3} \text{ y}^{-1}$ (case C) leads to a significant increase of actinides at about 10^3 years. A further decreased rate of $7 \cdot 10^{-4} \text{ y}^{-1}$ (case D) causes annual radiation exposures which are rather high compared to the reference case. In this case the initially bound actinide fraction of 98% of each actinide does not desorb significantly during transport, i.e. this curve represents an irreversibly sorbed actinide fraction. The shape of the curve is indeed very similar to the one shown in the case of actinides irreversibly bound on humic colloids. The most important radionuclides in this case are again ^{241}Am , ^{243}Am and ^{226}Ra .

However, this desorption rate is lower by a factor of 10^4 compared to the lowest values measured in laboratory.

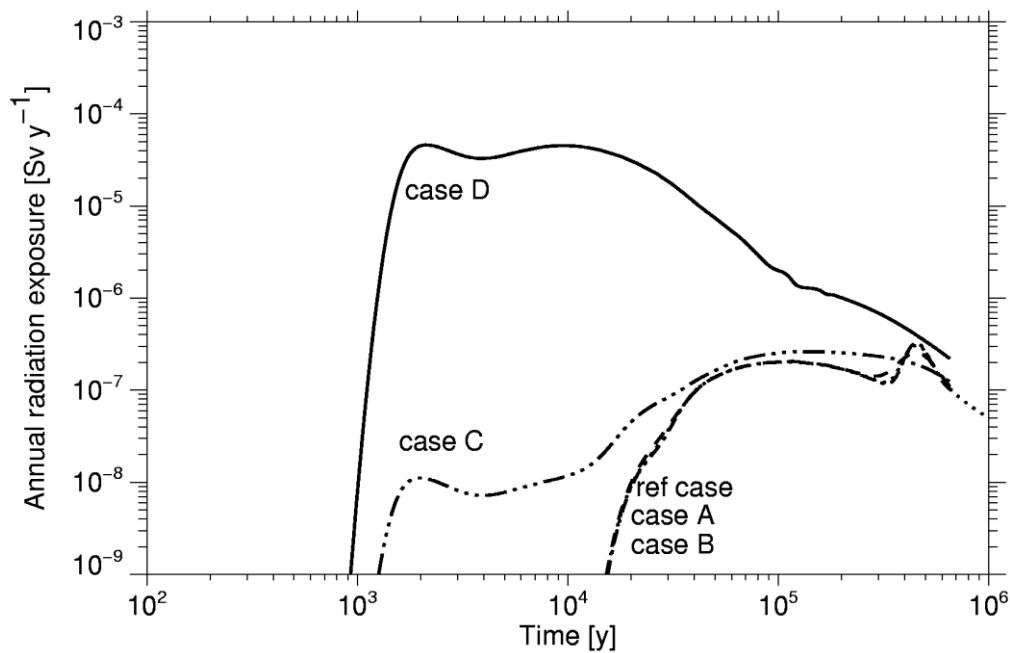


Figure 8: Annual radiation exposure for test cases with different desorption rates.
Case A: 7 y^{-1} ; case B: $7 \cdot 10^{-2} \text{ y}^{-1}$; case C: $7 \cdot 10^{-3} \text{ y}^{-1}$; case D: $7 \cdot 10^{-4} \text{ y}^{-1}$.

7. CONCLUSIONS

Column experiments with five different sediments are simulated with the transport code TRAPIC. The results confirm those received in previous investigations. Since the same groundwater was used in all experiments, the same input parameters were applied in all simulations with exception of the sorption values for Eu on the sediment. Important conclusions from the simulations are:

- The observed migration behaviour can not be described by equilibrium models. Kinetically controlled sorption mechanisms for the contaminants have to be considered.
- The main fraction of europium exists as Eu-humate and migrates through the column without retardation.
- Recoveries of less than 100 % are due to desorption of Eu from the colloids followed by sorption to the sediment matrix. A contribution of irreversible colloid filtration can not be ruled out.

- The rates for desorption of europium from the colloids decrease exponentially with increasing transport time.

Reversible colloid-sediment-interactions explain the tailing of the breakthrough curves. Assuming a constant ratio between mobile and immobile colloids good agreement is reached between simulated and experimentally obtained breakthrough curve. The capture rates of the colloids obtained by best fits increase with increasing Darcy-velocity. The values are in the same order of magnitude as calculated by filtration theory.

With regard to performance assessment, especially the mechanism of Eu desorption from the colloids has to be further investigated. This is a basis for scaling up desorption rates obtained from experiments of a few days duration to time periods of years. However, first calculations for a performance assessment were carried out regarding firstly, the lowest desorption rate measured in laboratory and secondly, an irreversibly bound fraction of actinides.

For typical groundwater velocities in the order of 1 m y^{-1} and transport pathway lengths of some thousand meters, as it is expected in typical aquifers in the overburden of potential repository sites, the desorption of actinides from humic colloids measured in laboratory is so fast, that it can be described as an equilibrium process. Even a decrease of the desorption rate by a factor of 100 has no influence on the PA calculation results.

At the moment, it cannot be ruled out that part of the actinides is irreversibly bound to humic colloids and that the colloids travel over long distances without retardation. This is of major importance, since short travel times strongly enhance the radiation exposure of short-lived radionuclides. In PA calculations assuming an irreversibly humic colloid bound actinide fraction of 45 %, ^{241}Am and ^{243}Am with half-lives of 432 years, and 3300 years, respectively, become the most important radionuclides for the radiation exposure. These nuclides did not play a role in long-term safety assessment studies up to now, since the assumption of high K_d -values causes long travel times and a strong decay before reaching the biosphere.

However, the presented calculations are based on assumptions that

- colloids are stable over more than 1000 years and are transported without filtration or retardation over distances of about 10 000 m and
- a high amount of actinides is initially bound to humic colloids. It is questionable, whether such a high amount of actinides will be directly sorbed onto actinides at the beginning of the transport pathway in the far field, since radionuclides squeezed out from a salt dome are dissolved in nearly saturated brines. Under these conditions colloids are usually not stable and coagulate.

ACKNOWLEDGEMENTS

This work has been partially financed by the Federal Ministry for Economy and Technology (BMW).

REFERENCES

1. Degueldre, C., Triay, I., Kim, J.I., Vilks, P., Laaksoharju, M., Miekeley, N.: Groundwater colloid properties: a global approach. *Applied Geochemistry* 15 (2000a) 819-832
2. Mc Carthy, J.P., Sanford, W.E., Stafford, P.L.: Lanthanide Field Tracers Demonstrate Enhanced Transport of Transuranic Radionuclides by Natural Organic Matter. *Environmental Science and Technology*, 32, (1998) 3901-3906.

3. Buckau, G., Artinger, R., Geyer, S., Wolf, W., Fritz, P., Kim, J.I.: Groundwater in-situ generation of aquatic humic and fulvic acids and the mineralization of sedimentary organic carbon. *Applied Geochemistry* 15 (2000a) 819-832.
4. Buckau, G., Artinger, R., Kim, J. I., Geyer, S., Fritz, P., Wolf, M., Frenzel B.: Development of climatic and vegetation conditions and the geochemical and isotopic composition in the Franconian Albvorland aquifer system. *Appl. Geochem.* 15 (2000c) 1191-1201
5. Artinger, R., Kienzler, B., Schüßler, W., Kim, J.I.: Effects of humic substances on the ²⁴¹Am migration in a sandy aquifer: Column experiments with Gorleben groundwater/sediment systems. *Journal of Contaminant Hydrology*, 35 (1998) 261-275.
6. Artinger, R., Seibert, A., Marquardt, C., Trautmann, N., Kratz, J. V., Kim J. I.: Humic colloid-borne Np migration: Influence of the oxidation state. *Radiochim. Acta* 88 (2000) 609-612.
7. Lührmann, L., Klotz, D., Knabner, P., Noseck, U.: Simulation der Eu-humat Migration mit dem Rechencode TRAPIC. in: "Geochemische Modellierung - Radiotoxische und chemisch-toxische Stoffe in natürlichen aquatischen Systemen." FZK-Bericht FZKA6051, Karlsruhe 1998.
8. Klotz, D., Lazik, D.: in *Colloid Migration in Groundwaters: Geochemical Interactions of Radionuclides with Natural Colloids*. EUR 16754 EN, pp 169-232 European Commission, Brussels, 1996.
9. Klotz, D., and Wolf M.: ¹⁵²Eu migration experiments with different sediments and flow velocities. Pages 367-372 in G. Buckau, editor. *Effects of humic substances on the migration of radionuclides: complexation and transport of actinides*. Third technical progress report. FZKA 6524, Karlsruhe 2000.
10. Noseck, U., Schuessler, W.: Impact of humic colloids on actinide migration with regard to performance assessment. Contribution for the Conference "Chemistry and Migration behaviour of actinides and fission products in the geosphere. Migration '01", Bregenz 16.-21, September 2001, To be published.
11. Buhmann, D., Nies, A., Storck, R.: Analyse der Langzeitsicherheit von Endlagerkonzepten für wärmeerzeugende radioaktive Abfälle. GSF-Bericht 27/91. GSF - Forschungszentrum für Umwelt und Gesundheit GmbH, Braunschweig 1991.
12. Lührmann, L., Noseck, U., Tix, C.: Model of contaminant transport in porous media in the presence of colloids applied to actinide migration in column experiments. *Water Resource Research* 34/3, 421-426, 1998.
13. Lührmann, L., Klotz, D., Knabner, P., Noseck, U.: Modellierung des kolloidgetragenen Stofftransports angewandt auf Eu-Humat-Migrationsexperimente. in: "Uranium Mining and Hydrogeology II." Proceedings of the International Conference and Workshop, Freiberg, September 1998.
14. Tien, C., Turian, R. M., Oendse, H.: Simulation of the dynamic behaviour of deep bed filters. *AIChE J.* 25, 385-395 (1979).
15. Yao, K. M., Habibian, T., O'Melia, Ch. R.: *Water and Waste Water Filtration: Concepts and Applications*. *Environmental Science and Technology* 5, 1105-1112 (1971).
16. Schüßler W., Artinger, R. Kienzler, B., Kim, J.I.: Conceptual Modeling of the Humic Colloid Borne Americium Migration by a Kinetic Approach. *Environmental Science and Technology* 34, 2608-2611 (2000).
17. Geckeis, H., Rabung, T., Kim, J. I.: Kinetic Aspects of the Metal Ion Binding to Humic Substances. Pages 47-58 in G. Buckau, editor. *Effects of humic substances on the migration of radionuclides: complexation and transport of actinides*. Second technical progress report. FZKA 6324, Karlsruhe 1999.

18. Grauer, R.: Zur Chemie von Kolloiden: Verfügbare Sorptionsmodelle und zur Frage der Kolloidhaftung. Paul Scherrer Institut, PSI-Bericht Nr. 65, 1990.